Inorganic Chemistry
Communication
pubs.acs.org/IC

Coordination Chemistry of Single-Site Catalyst Precursors in Reductively Electropolymerized Vinylbipyridine Films

Daniel P. Harrison,[†] Alexander M. Lapides,[‡] Robert A. Binstead,[‡] Javier J. Concepcion,[‡] Manuel A. Méndez,[‡] Daniel A. Torelli,[‡] Joseph L. Templeton,[‡] and Thomas J. Meyer*,[‡]

[†]Department of Chemistry, Virginia Military Institute, Lexington, Virginia 24450, United States

[‡]Department of Chemistry, University of North Carolina at Chapel Hill, CB 3290, Chapel Hill, North Carolina 27599-3290, United States

S *Supporting Information*

ABSTRACT: Reductive electropolymerization of $[Ru^{II}(PhTpy)(5,5'\text{-dvbpy})(Cl)](PF_6)$ and $[Ru^{II}(PhTpy)(5,5'\text{-dvbpy})(MeCN)](PF_6)_2$ (PhTpy is 4′-phenyl-2,2′:6′,2″-terpyridine; 5,5′-dvbpy is 5,5′-divinyl-2,2′-bipyridine) on glassy carbon electrodes gives well-defined films of poly$\{[Ru^{II}(PhTpy)(5,5'\text{-dvbpy})(Cl)](PF_6)\}$ (poly-**1**) or poly$\{[Ru^{II}(PhTpy)(5,5'\text{-dvbpy})(MeCN)](PF_6)_2\}$ (poly-**2**). Oxidative cycling of poly-**2** with added NO_3^- results in the replacement of coordinated MeCN by NO_3^- to give poly$\{[Ru^{II}(PhTpy)(5,5'\text{-dvbpy})(NO_3)]^+\}$, and with 0.1 M $HClO_4$, replacement by H_2O occurs to give poly$\{[Ru^{II}(PhTpy)(5,5'\text{-dvbpy})(OH_2)]^{2+}\}$ (poly-$\mathbf{OH_2}$). Although analogous aqua complexes (e.g., $[Ru(tpy)(bpy)(OH_2)]^{2+}$) undergo rapid loss of H_2O to MeCN in solution, poly-$\mathbf{OH_2}$ and poly-$\mathbf{OH_2}^+$ are substitutionally inert in MeCN. The substitution chemistry is reversible, with reductive scans of poly-**1** or poly-$\mathbf{OH_2}$ in MeCN resulting in poly-**2**, although with some loss of Faradaic response.

Well-established procedures are available for the electropolymerization of vinyl-[1] and pyrrole-derivatized[2] metal complexes on a variety conducting substrates. The electron transfer,[1b,i] photochemical,[1c,e,j] diffusional,[2b] and related properties of the resulting films, including electrocatalysis,[1f−h,2a,d] have also been investigated. Electropolymerization offers significant advantages over other approaches to modifying surfaces. With multiple polymerizable functional groups, cross-linking and formation of relatively high polymers lead to film formation by physical adsorption to the electrode surface. The resulting interfacial film structures are stable in a variety of media and over an extended pH range in water. This is in contrast to surface binding to oxides by carboxylate- or phosphonate-derivatized complexes, the former of which are unstable on oxide surfaces in water and the latter at elevated pHs.[3]

A particular target for us is to design interfaces for electrocatalytic and photoelectrocatalytic applications. In one strategy, electropolymerization is used to form films from monomer-based catalyst precursors; recent examples have appeared based on oxidatively induced pyrrole polymerization.[2c,d] Here we report our initial findings on reductive electropolymerization of the catalyst precursor complexes $[Ru^{II}(PhTpy)(5,5'\text{-dvbpy})(Cl)](PF_6)$ (**1**) and $[Ru^{II}(PhTpy)(5,5'\text{-dvbpy})(MeCN)](PF_6)_2$ (**2**), where PhTpy is 4′-phenyl-2,2′:6′,2″-terpyridine and 5,5′-dvbpy is 5,5′-divinyl-2,2′-bipyridine (Figure 1), and the behavior of the resulting interfacial films, poly-**1** and poly-**2**. Earlier strategies relied on multiple polymerizable ligands and cross-linking, which limited the generality of the coordination chemistry. We report here that the doubly derivatized 5,5′-dvbpy ligand in these complexes is sufficient to achieve stable interfacial film structures, as reported earlier by Nie and co-workers.[4]

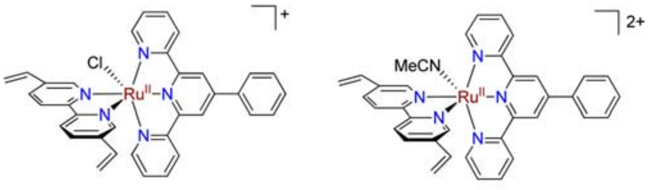

1 **2**

Figure 1. Structures of single-site ruthenium complex catalyst precursors to poly-**1** and poly-**2**.

Electropolymerization of **1** and **2** to give poly-**1** and poly-**2** was induced by controlled potential electrolysis or cyclic voltammetric (CV) scans at (or to) potentials sufficiently negative to reduce the ligands and initiate polymerization (Figure S1, Supporting Information, SI). Either technique produces surface coverages (Γ in mol/cm^2; see eqs S1 and S2, SI) that increase linearly with the number of reductive scan cycles or with time (Figures S2 and S3, SI). Electropolymerized films of poly-**1** ($Ru^{III/II}$: $E_{1/2}$ = +0.56 V vs $Ag/AgNO_3$[5] and −0.094 V vs $FeCp_2^{+/0}$) and poly-**2** ($Ru^{III/II}$: $E_{1/2}$ = +0.99 V vs $Ag^{+/0}$) on 0.071 cm^2 glassy carbon electrodes (GCEs) in 0.1 M $[TBA]PF_6$/MeCN ($[TBA]PF_6$ is tetra-*n*-butylammonium hexafluorophosphate) display peak-to-peak separations (ΔE_p) of 22 and 21 mV (Figure S4, SI), respectively, at a scan rate, ν, of 100 mV/s. ΔE_p approaches 0 as the scan rate is decreased, as expected for a surface wave (Figure S5, SI). UV−vis spectra of poly-**1** and poly-**2** on semitransparent fluorine-doped tin oxide (FTO) surfaces closely resemble those of **1** and **2** in solution (Figures S6 and S7, SI).

Received: November 12, 2012
Published: April 24, 2013

dx.doi.org/10.1021/ic302472r | *Inorg. Chem.* 2013, 52, 4747−4749

Oxidatively Induced Ligand Substitution. Oxidatively cycling poly-**2** through the $Ru^{III/II}$ wave in a 1 mM solution of $[TBA]NO_3$ (in 0.1 M $[TBA]PF_6$/MeCN) produces a new surface couple at $E_{1/2} = +0.68$ V (Figure 2). Interconversion from poly-**2** to the new couple is complete after 20 scans from 0 to +1.5 V (Figure S8, SI). A characteristic prewave appears at $E_{p,c} = +0.80$ V because of changes in the film structure arising from ion transport.[6] The negative shift of $\Delta E_{1/2} = -0.34$ V is consistent with oxidation to Ru^{III}, followed by substitution of MeCN by NO_3^- to give poly-$Ru^{III}ONO_2^{2+}$ (poly-$\mathbf{ONO_2}^+$; eqs 1 and 2). UV−vis spectral data are consistent with this conclusion (Figure S9A, SI). Oxidatively induced substitution of MeCN for NO_3^- in $Ru(tpy)(bpy)(NCMe)^{2+}$ also occurs in solution under the same conditions.

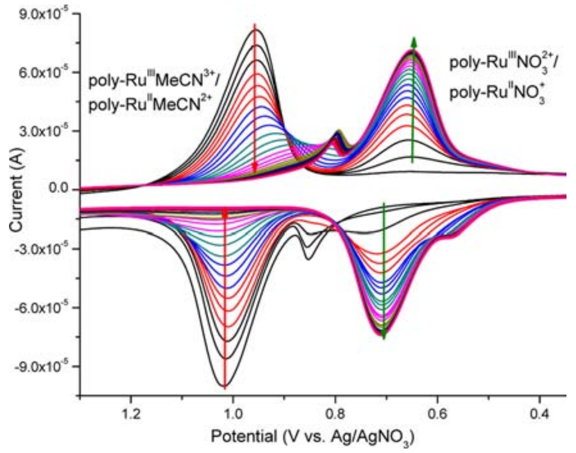

Figure 2. Oxidative CVs of poly-**2** on a GCE in 1 mM $[TBA]NO_3$ (ν = 250 mV/s), illustrating the loss of poly-**2** (red arrows; $\Gamma = 3.7 \times 10^{-9}$ mol/cm^2) and the appearance of poly-$\mathbf{ONO_2}$ (green arrows). The shoulder at +0.55 V vs $Ag/AgNO_3$ appears to be poly-$\mathbf{OH_2}$, arising from trace water in the initial solution (see below).

$$\text{poly-Ru}^{II}\text{NCMe}^{2+} \xrightarrow{-e^-} \text{poly-Ru}^{III}\text{NCMe}^{3+} \tag{1}$$

$$\text{poly-Ru}^{III}\text{NCMe}^{3+} + NO_3^- \rightarrow \text{poly-Ru}^{III}\text{ONO}_2{}^{2+} + \text{MeCN} \tag{2}$$

The poly-$Ru^{III}ONO_2^{2+}$ couple was not present following a single oxidative sweep of 0 → 1.5 V or after soaking of a GCE−poly-**2** electrode in $[TBA]NO_3$ for 72 h. There was no sign of coordination of HSO_4^-, ClO_4^-, or OTf$^-$ by oxidative cycling of poly-**2** under comparable conditions. Cl^- is preferred over NO_3^- in the coordination spheres of both Ru^{III} and Ru^{II}. There was no evidence for substitution of Cl^- for NO_3^- in poly-**1**. In MeCN 5 mM in Cl^-, substitution of NO_3^- occurs, converting poly-$\mathbf{ONO_2}^+$ to poly-**1** by the reaction, poly-$Ru^{III}ONO_2^{2+}$ + Cl^- → poly-**1** + NO_3^- with oxidative cycling with slow substitution (hours) occurring without cycling.

Similarly, oxidative cycling of poly-**2** in 0.1 M $HClO_4$ between 0 and +1.5 V gives poly-$Ru^{III}OH_2^{3+}$ (poly-$\mathbf{OH_2}^+$; eqs 1 and 3), with $E_{1/2} = +0.80$ V compared to $E_{1/2} = +0.79$ V vs SCE for the $[Ru(bpy)(bpy)OH_2]^{3+/2+}$ couple at pH 1 (Figure 3).[7] UV−vis spectral data corroborate these results (Figure S10, SI). The reaction is complete after 20 cycles (Figure S11, SI). There was no sign of aquation when poly-**2** was soaked in 0.1 M $HClO_4$ for 72 h. Careful inspection of the scan sequence in Figure 3 reveals that a smaller wave at $E_{1/2} \sim 0.68$ V appears during the first few scan cycles. This wave may arise from sites near the film−solution interface that undergo substitution more rapidly than sites in the film interior.

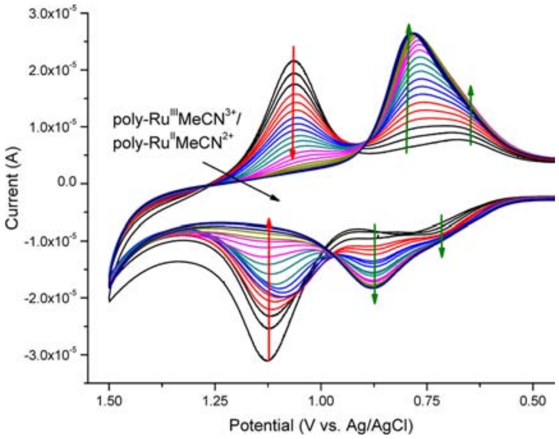

Figure 3. Formation of poly-$\mathbf{H_2O}$ following oxidative scan cycles of poly-**2** (red arrows; $\Gamma_{initial} = 2.7 \times 10^{-9}$ mol/cm^2) in 0.1 M $HClO_4$; GCE, 0.071 cm^2, ν = 100 mV/s.

$$\text{poly-Ru}^{III}\text{NCMe}^{3+} + H_2O \rightarrow \text{poly-Ru}^{III}\text{OH}_2{}^{3+} + \text{MeCN} \tag{3}$$

Appearance of the aqua complex is significant given the known pH-dependent proton-coupled electron-transfer (PCET) properties of $[Ru(tpy)(bpy)(OH_2)]^{2+}$ and the oxidative reactivity of higher-oxidation-state $Ru^{IV}(O)$ and $Ru^{V}(O)$ forms.[3,8] The film-based redox chemistry is currently under investigation. In MeCN, $[Ru(tpy)(bpy)(OH_2)]^{2+}$ undergoes substitution of H_2O by MeCN in minutes. By contrast, there is no evidence for poly-**2** when poly-$\mathbf{H_2O}$ is soaked in $[TBA]PF_6$/MeCN for extended periods or after oxidative cycling. NO_3^- is lost from poly-$\mathbf{ONO_2}$ to give poly-$\mathbf{H_2O}$ upon oxidative cycling in 0.1 M $HClO_4$ or upon soaking in 0.1 M $HClO_4$. It is noteworthy that the substitution kinetics of MeCN in poly-**2** for OH_2 or NO_3^- are zero-order over an extensive dynamic range consistent with a noncomplex rate-limiting step, namely, diffusion into the film (Figures S8 and S11, SI).

Reductively Induced Substitution. Ligand substitution is also induced by reductive cycling following reduction at the π^*(polypyridyl) levels of the ligands. The results of three reductive scan cycles of poly-**1** at 100 mV/s in 0.1 M $[TBA]PF_6$/MeCN at 0 → −1.97 V under N_2 are shown in Figure 4a.[9] On the first scan, a prewave appears at $E_{p,c} = -1.27$ V followed by surface waves at $E_{1/2} = -1.66$ V (PhTpy reduction) and at $E_{1/2} = -1.87$ V (5,5′-poly-vbpy reduction).

Following the first scan through both ligand-based reductions, a new surface-based couple appears at $E_{p,c} = -1.49$ V, which coincides with $E_{p,c}$ for the first PhTpy-based reduction in poly-**2**. A subsequent oxidative scan and the appearance of a wave at $E_{1/2}$ = +1.02 V for the poly-$Ru^{III}NCMe^{3+/2+}$ couple reveals that ligand-based reduction induces conversion of poly-**1** into poly-**2** (eqs 4 and 5; Figures 4b and S12 and S13, SI). UV−vis spectral data corroborate these results (Figure S14, SI). The substitution mechanism, following π^*(PhTpy)/π^*(5,5′-poly-vbpy) reduction, is presumably by thermal population of ruthenium-based $d\sigma^*$ levels, which induces ligand labilization.

$$\text{poly-RuCl}^{+} + 2e^- + \text{MeCN} \rightarrow \text{poly-RuNCMe}^{0} + Cl^- \tag{4}$$

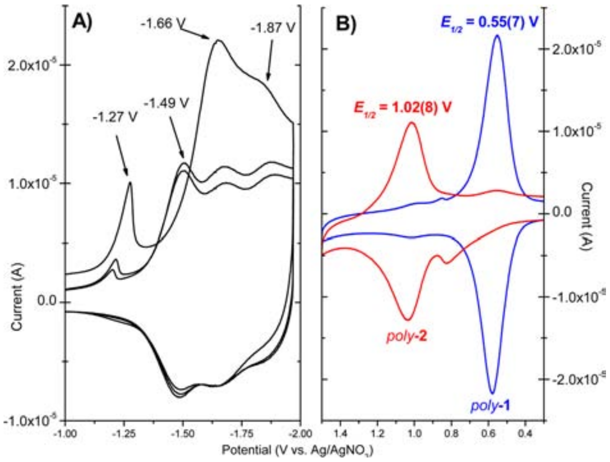

Figure 4. (A) Reductive CVs of poly-**1** under N_2 (black). (B) Oxidative CVs of a poly-**1** electrode prior to reductive cycling (blue; $\Gamma = 1.7 \times 10^{-9}$ mol/cm^2) and after reductive cycling (red). Both parts A and B were obtained in fresh solutions of 0.1 M [TBA]PF_6/MeCN after electropolymerization on a 0.071 cm^2 GCE.

$$\text{poly-RuNCMe}^0 - 2e^- \rightarrow \text{poly-RuNCMe}^{2+} \qquad (5)$$

Ligand-based reduction and substitution are accompanied by a loss of Faradaic response, with $\Gamma = 1.7 \times 10^{-9}$ mol/cm^2 for the initial poly-**1** $Ru^{III/II}$ wave at $E_{1/2}$ = +0.56 V decreasing to $\Gamma = 9.3 \times 10^{-10}$ mol/cm^2 for the poly-**2** wave at $E_{1/2}$ = +1.03 V. In addition, a new, distorted prewave appears at $E_{p,a}$ = +0.82 V (Figure 4b). This observation points to a 46% decrease in the redox response at the end of three reductive scan cycles. A related response was observed for a thinner film of poly-**1** with $\Gamma = 4.5 \times 10^{-10}$ mol/cm^2 before a reductive cycle and $\Gamma = 3.2 \times 10^{-10}$ mol/cm^2 for poly-**2**, a 29% loss. Reductive cycling of poly-**ONO_2** and poly-**H_2O** both result in poly-**2** with comparable decreases in Γ (Figures S15 and S16, SI). The loss mechanism is currently under investigation. It is noteworthy that, after the initial exchange occurs with a loss of electroactivity, further decreases are greatly ameliorated upon additional reductive scan cycles (Figure S13, SI).

Our results are important in revealing systematic and synthetically exploitable features in the film-based coordination chemistries of poly-**1** and poly-**2** with significant differences between film and solution behavior. Polypyridyl complexes of dπ^6 Ru^{II} typically undergo slow loss of nitrile ligands. Nitrile ligands are weak σ donors and derive coordinative stability from $d_\pi - \pi^*$ back-bonding from Ru^{II}. With oxidation to Ru^{III}, back-bonding stabilization is no longer a factor, and nitriles become good leaving groups. Nitrile labilization was exploited here to convert poly-**2** into poly-**ONO_2** and poly-**OH_2**.

The film environment also plays an important role. Following conversion of poly-**2** into poly-**OH_2**, there is no sign of substitution of H_2O for MeCN in poly-**OH_2** or poly-$Ru^{III}OH_2^{3+}$ even over extended soaking or oxidative cycling periods in MeCN. This is a potentially important observation for possible applications in organic electrocatalysis based on Ru=O forms of poly-**OH_2** with MeCN as the external solvent.[9] Oxidatively induced anation and aquation provide a basis for systematic manipulation of the coordination environment at the redox-active Ru^{II} sites in films. Ligand-based reduction offers a route to loss of anions or water in MeCN to return the films to the initial poly-**2** state.

■ ASSOCIATED CONTENT

Ⓢ Supporting Information

Detailed experimental procedures, synthetic procedures, NMR spectra, Figures S1−S22, additional acknowledgments, and equations. This material is available free of charge via the Internet at http://pubs.acs.org.

■ AUTHOR INFORMATION

Corresponding Author

*E-mail: tjmeyer@unc.edu.

Notes

The authors declare no competing financial interest.

■ ACKNOWLEDGMENTS

D.P.H. acknowledges support from the U.S. Department of Energy Office of Science, Office of Basic Energy Sciences, under Award DE-FG02-06ER15788 and the Virginia Military Institute. A.M.L., R.A.B., and J.J.C. acknowledge support from the UNC Energy Frontier Research Center (EFRC): Center for Solar Fuels, an Energy Frontier Research Center funded by the U.S. Department of Energy, Office of Science, Office of Basic Energy Sciences, under Award DE-SC0001011.

■ REFERENCES

(1) (a) Calvert, J. M.; Schmehl, R. H.; Sullivan, B. P.; Facci, J. S.; Meyer, T. J.; Murray, R. W. *Inorg. Chem.* **1983**, *22*, 2151−2162. (b) Gould, S.; Gray, K. H.; Linton, R. W.; Meyer, T. J. *Inorg. Chem.* **1992**, *31*, 5521−5525. (c) Devenney, M.; Worl, L. A.; Gould, S.; Guadalupe, A.; Sullivan, B. P.; Caspar, J. V.; Leasure, R. L.; Gardner, J. R.; Meyer, T. J. *J. Phys. Chem. A* **1997**, *101*, 4535−4540. (d) Moss, J. A.; Argazzi, R.; Bignozzi, C. A.; Meyer, T. J. *Inorg. Chem.* **1997**, *36*, 762−763. (e) Moss, J. A.; Yang, J. C.; Stipkala, J. M.; Wen, X.; Bignozzi, C. A.; Meyer, G. J.; Meyer, T. J. *Inorg. Chem.* **2004**, *43*, 1784−1792. (f) O'Toole, T. R.; Margerum, L. D.; Westmoreland, T. D.; Vining, W. J.; Murray, R. W.; Meyer, T. J. *J. Chem. Soc., Chem. Commun.* **1985**, 1416−1417. (g) Ramos Sende, J. A.; Arana, C. R.; Hernandez, L.; Potts, K. T.; Keshevarz-K, M.; Abruna, H. D. *Inorg. Chem.* **1995**, *34*, 3339−3348. (h) Cosnier, S.; Deronzier, A.; Moutet, J.-C. *J. Mol. Catal.* **1988**, *45*, 381−391. (i) Abruna, H. D.; Denisevich, P.; Umana, M.; Meyer, T. J.; Murray, R. W. *J. Am. Chem. Soc.* **1981**, *103*, 1−5. (j) Yang, J.; Sykora, M.; Meyer, T. J. *Inorg. Chem.* **2005**, *44*, 3396−3404.

(2) (a) Cosnier, S.; Deronzier, A.; Moutet, J.-C. *J. Electroanal. Chem. Interfacial Electrochem.* **1986**, *207*, 315−321. (b) Deronzier, A.; Eloy, D.; Jardon, P.; Martre, A.; Moutet, J.-C. *J. Electroanal. Chem.* **1998**, *453*, 179−185. (c) Mola, J.; Mas-Marza, E.; Sala, X.; Romero, I.; Rodríguez, M.; Viñas, C.; Parella, T.; Llobet, A. *Angew. Chem., Int. Ed.* **2008**, *47*, 5830−5832. (d) Cheung, K.-C.; Guo, P.; So, M.-H.; Zhou, Z.-Y.; Lee, L. Y. S.; Wong, K.-Y. *Inorg. Chem.* **2012**, *51*, 6468−6475.

(3) (a) Concepcion, J. J.; Jurss, J. W.; Brennaman, M. K.; Hoertz, P. G.; Patrocinio, A. O. v. T.; Murakami Iha, N. Y.; Templeton, J. L.; Meyer, T. J. *Acc. Chem. Res.* **2009**, *42*, 1954−1965. (b) Chen, Z.; Concepcion, J. J.; Jurss, J. W.; Meyer, T. J. *J. Am. Chem. Soc.* **2009**, *131*, 15580−15581.

(4) Nie, H.-J.; Shao, J.-Y.; Wu, J.; Yao, J.; Zhong, Y.-W. *Organometallics* **2012**, *31*, 6952−6959.

(5) Silver wire reference electrode solution: 0.01 M $AgNO_3$, 0.1 M [TBA]PF_6, MeCN solution; −0.094 V vs $FeCp_2$.

(6) Abruña, H. D. *Coord. Chem. Rev.* **1988**, *86*, 135−189.

(7) Takeuchi, K. J.; Thompson, M. S.; Pipes, D. W.; Meyer, T. J. *Inorg. Chem.* **1984**, *23*, 1845−1851.

(8) (a) Meyer, T. J.; Huynh, M. H. V. *Inorg. Chem.* **2003**, *42*, 8140−8160. (b) Gagliardi, C. J.; Vannucci, A. K.; Concepcion, J. J.; Chen, Z.; Meyer, T. J. *Energy Environ. Sci.* **2012**, *5*, 7704−7717.

(9) Vanucci, A. K.; Chen, Z.; Concepcion, J. J.; Meyer, T. J. *ACS Catal.* **2012**, *2*, 716−719.